

Reactions of Triplet Diphenylcarbene by Hydrogen Atom Tunneling in Rigid Media¹

Matthew S. Platz,^{*2} V. P. Senthilnathan, Bradford B. Wright, and C. W. McCurdy, Jr.^{*2}

Contribution from the Department of Chemistry, The Ohio State University, Columbus, Ohio 43210. Received February 22, 1982

Abstract: Photolysis of diphenyldiazomethane in six matrices (toluene, methylcyclohexane, benzene, diethyl ether, 2-propanol, and cyclohexane) and their deuterated modifications at low temperature gave rise to the metastable triplet ESR spectrum of diphenylcarbene. Chemical and kinetic isotope effects established that the mechanism of the signal decay was hydrogen atom abstraction by the triplet ground state of diphenylcarbene from the matrix host. Analysis of the decay kinetics revealed that this process occurs by quantum mechanical tunneling of the hydrogen atom. Calculations based upon an Eckart barrier potential reproduced the experimental rate constants faithfully and gave reasonable values for the barrier width and height parameters. It was found that the signal decay in proton and perdeuterated matrices corresponded to sites of very different reactivity. The implications of the tunnel effect for the chemistry observed in low-temperature matrices are discussed.

Introduction

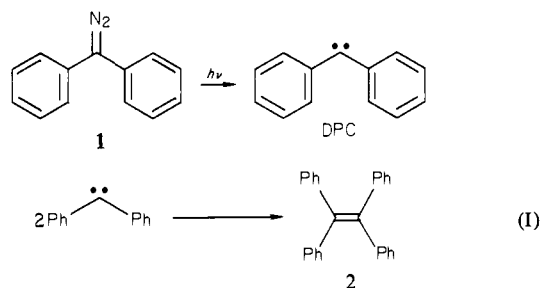
Diphenylcarbene (DPC) is one of the most extensively studied carbene intermediates. A wealth of chemical trapping studies has revealed the presence of two reactive states, the low-lying singlet, and the ground-state triplet.³ Chemical,⁴ spectroscopic,⁵ and kinetic⁶ studies of DPC indicate that the singlet-triplet energy gap is 5.1 ± 1 kcal/mol in acetonitrile and approximately 3 kcal/mol in benzene.

Recent studies of Moss⁷ and Tomioka and Griffin⁸ dealt with the chemistry of aryl carbenes in polycrystalline and glassy matrices at 77 K. Several differences between the solution and matrix chemistry were noted which were attributed to the large changes in temperature and phase. These observations prompted us to study the kinetics of triplet aryl carbenes in low-temperature matrices by electron spin resonance (ESR) spectroscopy.^{9,10} Based on the low Arrhenius parameters (both $\log A$ and the activation energy E_{act}) and the isotope effects observed, it was concluded that the mechanism of carbene decay was hydrogen atom abstraction via quantum mechanical tunneling. In this work we report more extensive studies of chemical and kinetic isotope effects and the results of tunneling calculations, which support our original interpretation.

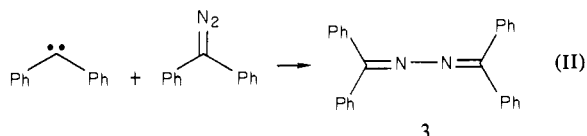
Matrix Chemistry and Kinetics of DPC

Matrix preparations of diphenyldiazomethane **1** were prepared by rapid cooling of dilute solutions of **1** in the solvent of choice. Brief photolysis (100 s) of the glass or polycrystal gave rise to the well known triplet ESR spectrum of DPC. The spectrum decayed immediately upon shuttering of the light source (Figure

1). The kinetics were obtained by measuring the signal intensity as a function of time. There are several possible decay reactions of DPC in the matrix. Conceivably DPC can dimerize to give tetraphenylethylene **2**.

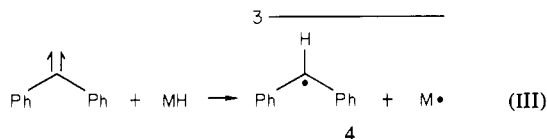


It can react with diazo compound **1** to give azine **3**

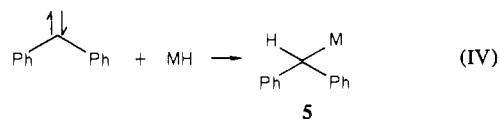


or it can react with trace amounts of water, oxygen, or other impurities.

In the case of a saturated solvent matrix it can react with a CH bond of the host. This will give rise to a radical pair **4**, in



the case of triplet DPC, and ultimately an adduct **5** as the isolated product. Smaller amount of products derived from disproportionation and symmetric radical-radical dimerization are also observed. Singlet DPC would likely directly insert into a CH bond to give adduct **5**, although radical-like reactions of singlet methylene have been detected by CIDNP.¹¹



Chemical analysis of aryl carbene matrix reactions are most consistent with reactions III or IV being the mechanism of the observed ESR signal decay. For example, Moss⁷ and Tomioka⁸ have shown that adducts such as **5** are the main reaction products in alkane, alkene, and alcohol matrices. Very little dimer or azine

(1) A preliminary account of this work has appeared. Wright, B. B.; Senthilnathan, V. P.; Platz, M. S.; McCurdy, C. W., Jr. *Tetrahedron Lett.* **1982**.

(2) Alfred P. Sloan Research Fellow.

(3) Trozzolo, A. M.; Wasserman, E. In "Carbenes", Vol. 2, Moss, R. A.; Jones, M., Jr., Ed.; Wiley: New York, 1975.

(4) (a) Closs, G. L. *Top. Stereochem.* **1968**, *3*, 193; (b) Bethell, D.; Stevens, G.; Tickl, P. *J. Chem. Soc. D* **1970**, 792; (c) Gaspar, P. P.; Whitsell, B. L.; Jones, M., Jr.; Lambert, J. B. *J. Am. Chem. Soc.* **1980**, *102*, 6108.

(5) Closs, G. L. In "Chemically Induced Magnetic Polarization"; Lepley, A. R.; Closs, G. L., Ed.; Wiley: New York, 1973.

(6) (a) Closs, G. L.; Robinson, R. E. *J. Am. Chem. Soc.* **1976**, *98*, 8190; (b) Eisenthal, K. B.; Turro, W. J.; Aikawa, M.; Butcher, J. A., Jr.; DuPuy, C.; Heffner, G.; Hetherington, W.; Korenowski, G. M.; McAuliffe, M. H. *Ibid.* **1980**, *102*, 6563.

(7) (a) Moss, R. A.; Joyce, M. A. *J. Am. Chem. Soc.* **1978**, *100*, 4475-4480; (b) Moss, R. A.; Huselton, J. K. *Ibid.* **1978**, *100*, 1314-1315; (c) Moss, R. A.; Joyce, M. A. *Ibid.* **1977**, *99*, 1262-1264; (d) Moss, R. A.; Dolling, U. H. *Ibid.* **1971**, *93*, 954-960.

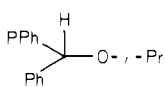
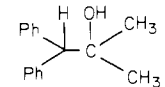
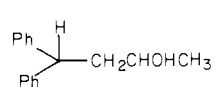
(8) (a) Tomioka, H.; Griffin, G. W.; Nishiyama, K. (b) Tomioka, H.; Inagaki, T.; Nakamura, S.; Izawa, Y. *J. Chem. Soc., Perkin Trans. 1* **1979**, 130-134; (c) Tomioka, H.; Izawa, Y. *J. Am. Chem. Soc.* **1977**, *99*, 6128-6129; (d) Tomioka, H. *J. Am. Chem. Soc.* **1979**, *101*, 256-257; (e) Tomioka, H.; Inagaki, T.; Izawa, Y. *J. Chem. Soc., Chem. Commun.* **1976**, 1023-1024; (f) Tomioka, H.; Ueda, H.; Kondo, S.; Izawa, Y. *J. Am. Chem. Soc.* **1980**, *102*, 7817.

(9) (a) Senthilnathan, V. P.; Platz, M. S. *J. Am. Chem. Soc.* **1980**, *102*, 7637; (b) Line, C. T.; Gaspar, P. P. *Tetrahedron Lett.* **1980**, 3553.

(10) Senthilnathan, V. P.; Platz, M. S. *J. Am. Chem. Soc.* **1981**, *103*, 5503.

(11) Roth, H. D. *J. Am. Chem. Soc.* **1971**, *93*, 1527.

Table I. Chemical and Kinetic Isotope Effects in the Reaction of Diphenylcarbene with Isotopically Labeled 2-Propanols at 77 K^a

matrix	$t_{1/20}$, min			
$\begin{array}{c} \text{OH} \\ \\ \text{CH}_3-\text{CHCH}_3 \\ \\ \text{OD} \end{array}$	6 ± 1	24.6	54.5	20.9
$\begin{array}{c} \text{CH}_3-\text{CHCH}_3 \\ \\ \text{OH} \end{array}$	7.5 ± 1	22.8	52.4	24.8
$\begin{array}{c} \text{CD}_3-\text{CHCD}_3 \\ \\ \text{OH} \end{array}$	20.5 ± 4	26.4	73.6	trace
$\begin{array}{c} \text{CH}_3-\text{CDCH}_3 \\ \\ \text{OD} \end{array}$	15 ± 3	45.1	13.6	41.3
$\text{CD}_3-\text{CD}_2\text{CD}_3$	2920 ± 45	67.9	32.1	trace

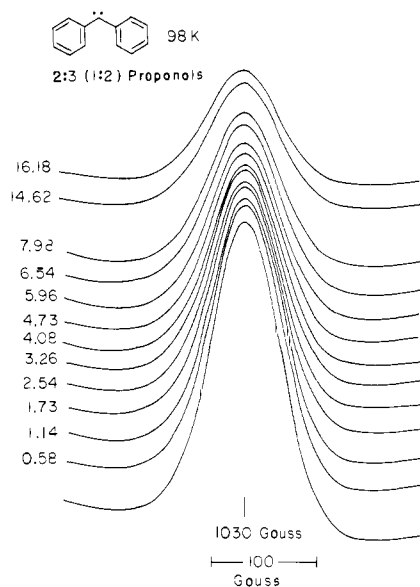
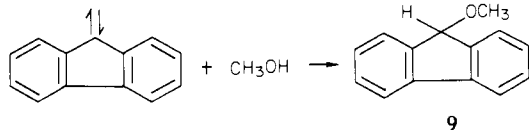
^a Product ratios are $\pm 2\%$.

Figure 1. The signal intensity of DPC in 2:3 (1:2) propanol glass at 98 K.

was found in the aforementioned aromatic carbene reactions at 77 K. However, care must be exercised as the extreme sensitivity of ESR can allow it to focus on a relatively slow, chemically insignificant process. More telling evidence against reactions I and II as the mechanism of the ESR signal decay process is provided by the observation of significant rate retardation upon perdeuteration of the matrix. One cannot predict a priori what magnitude of the isotope effect should be expected for reactions III and IV. Therefore, the data do not immediately rule out a small contribution of reactions I and II or reactions with impurities to the overall signal decay.

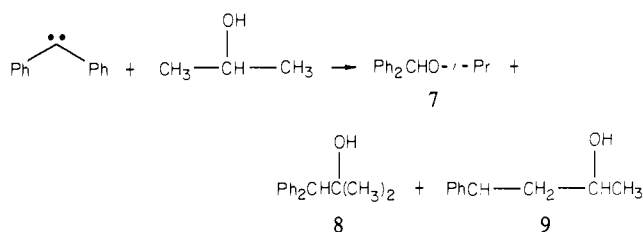
A more satisfying connection between the ESR kinetics and the bulk chemistry of a low-temperature sample is provided in a study of a series of isotopically labeled 2-propanols. Alcohols are excellent traps of singlet carbenes. Zupancic and Schuster have shown that fluorenylidene reacts with methanol at close to a diffusion-controlled rate to form ether 6.¹² Singlet DPC reacts with methanol at the diffusion rate.⁶



Triplet fluorenylidene and triplet 1-naphthyl carbene react with

(12) (a) Zupancic, J. J.; Schuster, G. B. *J. Am. Chem. Soc.* **1980**, *102*, 5958; (b) *Ibid.* **1981**, *103*, 944.

methanol at an appreciable rate in solution.^{12,13} This is a consequence of small singlet-triplet gaps and rapid spin equilibration. Previous work in low-temperature alcoholic matrices has revealed the formation of products due to carbene insertion into both the C-H and O-H positions.^{7,8}



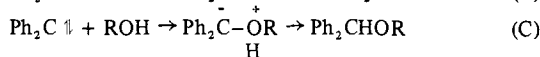
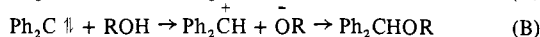
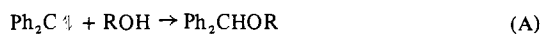
Brief photolysis (100 s) of a 10^{-1} M sample of **1** in 2-propanol at 77 K produces a strong ESR signal of triplet DPC. The time required for 5% of the triplet signal to decay in 2-propanol and in its deuterated modifications is listed in Table I. Within experimental error there is no OH(D) kinetic isotope effect. However, substantial CH(D) kinetic isotope effects are apparent in 2-propanol-2-*d*₁ and 2-propanol-1,1,1,3,3,3-*d*₆ matrices.

The kinetic results are entirely consistent with product isotope effects; 10^{-2} M solutions of diazo compound **1** in 2-propanol and its deuterated modifications were photolyzed at 77 K and stored in the dark at this temperature for 48 h to ensure complete carbene reactions prior to annealing the sample. Unreacted diazo compound was consumed by the addition of neat acrylonitrile before analysis by gas chromatography. The product distributions are reported in Table I. There is virtually no OH(D) product isotope effect but substantial CH(D) product isotope effects. In fact, the formation of primary CH insertion adducts is almost totally suppressed in *d*₆ alcohol, and the yield of tertiary CH insertion adducts is reduced by almost a factor of 5 in 2-propanol-2-*d*₁. The similarity between the kinetic and product isotope effects shows that the ESR method is not focusing on a minor chemical process but is representative of bulk chemistry of the sample. Based on the previously cited product studies of Moss et al.,^{7,8} the observed chemical and kinetic isotope effects, and the fact (to be discussed later) that the rate constants give good fits to tunneling calculations, it will be assumed that the ESR signal decay monitors a clean bimolecular reaction between the carbene and the matrix. Further evidence in support of this interpretation is provided by the observation that DPC is indefinitely stable in a more inert polycrystalline matrix, hexafluorobenzene, under identical experimental conditions.

The chemical and kinetic isotope data in 2-propanol also bear upon the question of which spin state of the carbene is responsible for reaction. The lack of an -OH(D) isotope effect immediately rules out abstraction of the OH hydrogen by triplet DPC as the mechanism of ether formation in the matrix. This is not surprising

(13) Hadel, L.; Platz, M. S.; Scaiano, J. C. *J. Am. Chem. Soc.*, in press.

in light of the large OH bond dissociation energy (103 kcal/mol).¹⁴ More significantly, this observation rules out certain decay mechanisms involving the low-lying singlet state. The exact mechanism of singlet insertion into an OH bond is not known for DPC. Three attractive possibilities are (A) a concerted insertion process, (B) proton transfer followed by ion pair collapse, or (C) ylid formation followed by proton migration.¹⁵



At 77 K processes A and B should be subject to a considerable primary isotope effect. This immediately rules out a mechanism involving rapid triplet \rightleftharpoons singlet equilibration followed by rate-determining proton abstraction or concerted insertion reactions of the low-lying singlet.

Eisenthal et al. have determined that the rate of S \rightarrow T intersystem crossing in DPC at 298 K is $k_{ST} = 9.1 \times 10^9 \text{ s}^{-1}$.^{6b} Indeed, the solution chemistry of DPC strongly indicates that spin interconversion in either direction is much faster than chemistry.³ This follows from the observation that direct and photosensitized photolysis of diazo compound **1** give the same product distributions, and do not show dilution effects. This circumstance is not likely to still hold in low-temperature matrices. If the singlet-triplet gap in DPC is as large as 3 kcal/mol, as is currently accepted,¹⁶ the equilibrium ratio of [S]/[T] at 77 K will be less than 10^{-8} . Doetschman has shown that $k_{ST} \geq 10^7 \text{ s}^{-1}$ even at 1.2 K.¹⁷ Thus if the energy gap is ≥ 3 kcal/mol, the rate constant in the reverse direction (k_{TS}) will be less than 10^{-2} s^{-1} at 77 K. This is as slow as or slower than the rate of matrix reactions as monitored by ESR.

In polycrystalline 2-propanol- d_8 , labeled ether **7** is formed in nearly 68% yield. The decay kinetics in this matrix are almost 500 times slower than in the parent alcohol. This indicates that in cases where DPC decay occurs predominantly through the low-lying singlet the rate is exceedingly slow. The polycrystalline matrices toluene, methylcyclohexane (MCH), diethyl ether, benzene, and cyclohexene all exhibit large kinetic isotope effects and much faster kinetics than the reaction with 2-propanol- d_8 . Considering that an authentic singlet reaction of DPC shows slow kinetics and minimal isotope effects and that the aforementioned substrates should be less reactive substrates for singlet DPC than an alcohol, it must be the ground triplet state of DPC which is responsible for the observed decay in toluene, MCH, ether, benzene, and cyclohexene via hydrogen atom abstraction (reaction III). This does not mean that all of the C-H insertion products observed in the bulk chemistry are triplet derived. Our data are permissive of some singlet-derived C-H adducts, but this process is not what we detect by kinetic ESR.

The instantaneous concentration of triplet DPC is less than 10^{-4} M in the matrix. This predicts that simple pseudo-first-order kinetics should be observed. However, a plot of $\log I$ vs. time (where I is the ESR signal intensity of the carbene) significantly deviates from linearity within relatively short reaction times (Figure 2). A plot of $\log I$ vs. $t^{1/2}$ (in polycrystals) gives excellent correlations.

Nonexponential decay of radicals¹⁸ in the solid state is a well-known phenomenon and has been attributed to a multiple

(14) Benson, S. W. "Thermochemical Kinetics"; Wiley: New York, 1968; p 215.

(15) For a recent study of singlet carbene reactions with alcohols, see Kirmse, W.; Loosen, K.; Sloma, H. D. *J. Am. Chem. Soc.* **1981**, *103*, 5935.

(16) The experimental measurements of singlet-triplet gaps are based on the following mechanistic assumption $^3\text{DPC} \rightleftharpoons ^1\text{DPC}_{\text{alcohol}}$ ether. Recent work by Scaiano suggests that this assumption may not be valid (personal communication from J. C. Scaiano).

(17) Doetschman, D. C. *J. Phys. Chem.* **1976**, *80*, 2167.

(18) (a) Sprague, E. D. *J. Phys. Chem.* **1973**, *77*, 2066-2070; (b) Neiss, M. A.; Willard, J. E. *Ibid.* **1975**, *79*, 783-791; (c) Neiss, M. A.; Sprague, E. D.; Willard, J. E. **1972**, *76*, 546-1121; (d) French, W. A.; Willard, J. E. *Ibid.* **1968**, *72*, 4604-4608; (e) Hudson, R. L.; Shiotan, M.; Williams, F. *Chem. Phys. Lett.* **1977**, *48*, 193-195.

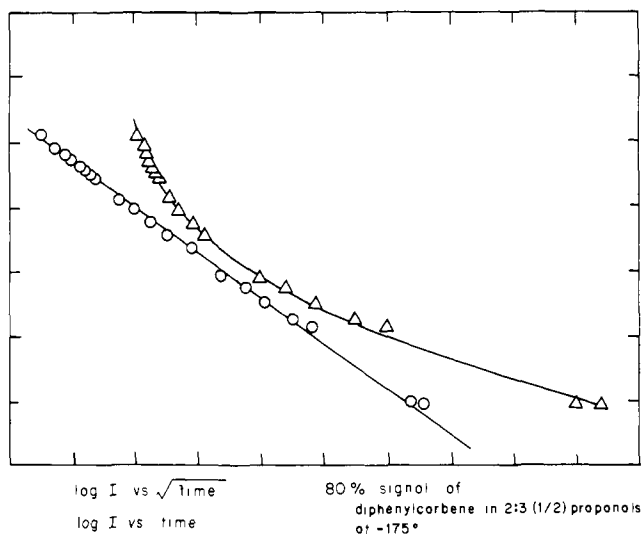
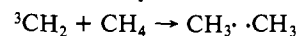


Figure 2. Plots of $\log [\text{DPC}]$ vs. time (Δ) and time^{1/2} (O) in 2:3 (1:2) propanol glass at 98 K over 80% of the ESR signal decay.

site problem. The free radicals and carbenes will be generated in a multitude of orientations relative to the host molecules. These sites will not interconvert in the matrix due to the low temperatures and high viscosities employed and their associated long molecular rotational relaxation times.

Schaefer¹⁹ has studied the potential surface for the reaction



The lowest energy barrier to reaction results when the methane hydrogen is in the plane of methylene, and it approaches the carbene center along the line which bisects the HCH bond angle. In a polycrystalline or glassy matrix the nascent carbenes will be locked into a variety of sites which differ in their proximity and orientation relative to matrix C-H bonds. Molecular nitrogen is also generated in the matrix photochemistry and may interfere with the reaction to a variable extent. Presumably each site in the matrix will be associated with a unique rate constant dependent upon the local environment.

Photolysis of the diazo-containing matrix for 100 s produces DPC in sites of widely varying reactivity. When the irradiation is discontinued the decay of highly reactive sites is measured. After these sites are depleted by reaction they are not regenerated. At this point the kinetic study focuses on less reactive sites until they too are depleted. In this fashion the observed pseudo-first-order rate constants (defined by tangents to the $\log I$ plot) should continuously decrease. A plot of $\log I$ vs. time is linear over brief periods of time. Over these abbreviated time intervals the kinetics are assumed to be associated with a single reactive site with a unique rate constant. Following this procedure one finds that the pseudo-first-order rate constants decrease by a factor of 3 to 4 over 80% of the decay of the carbene signal. This factor would certainly be larger if the kinetics of all matrix sites could be determined. However, during the 100 s of photolysis used to build up the DPC signal, extremely reactive sites are populated and then they decay faster than they can be measured. The decay of extremely unreactive sites cannot be measured with any degree of precision due to temperature drift.

The aforementioned $t^{1/2}$ rate law observed for DPC in glasses is well precedented. Bal'Shakov and Tolkachov have observed a $t^{1/2}$ dependence for the decay of alkyl radicals in glassy matrices.²⁰ A $t^{1/2}$ rate law has been derived by Förster for energy transfer between donor and acceptor species at variable distances.²¹

(19) Bauschlicher, C. N., Jr.; Bender, C. F.; Schaefer, H. F., III *J. Am. Chem. Soc.* **1976**, *98*, 3072.

(20) (a) Bol'Shakov, Z. V.; Tolkatchen, V. A. *Chem. Phys. Lett.* **1976**, *40*, 468-470; (b) Bol'Shakov, Z. V.; Fuks, M. P.; Tolkatchev, V. A.; Burstein, A. I. *Radiol. Chem. 4th* **1976**, *4*, 723-725.

(21) (a) Förster, Th. *Z. Naturforsch.* **1979**, *4a*, 3217; (b) Yardley, J. T. "Introduction to Molecular Energy Transfer"; Academic Press: New York, 1980; pp 239-241.

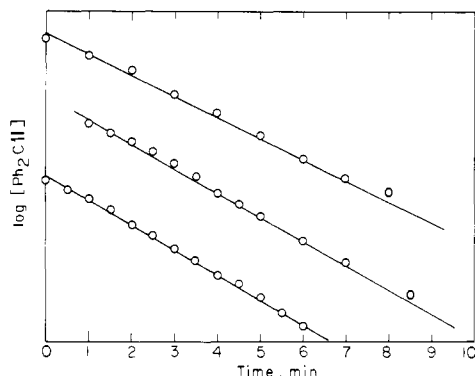
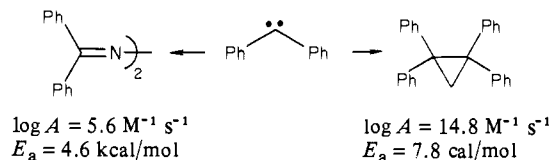


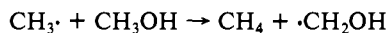
Figure 3. Initial decay plots of DPC in diethyl ether at 93 K. Only the decay of the initial 20% of the signal is analyzed.

If all of the carbenes could be prepared with the same orientation relative to the matrix host, clean first-order-kinetics would obtain. This circumstance has been observed previously. Doetschman and Hutchison have prepared a single crystal of 1,1-diphenylethylene **9** containing a small amount of diphenyldiazomethane. Photolysis of the crystal at 77 K produces a highly ordered ensemble of triplet DPC. Clean first-order kinetics were observed for the reaction of DPC with 1,1-diphenylethylene or diphenyldiazomethane.²²

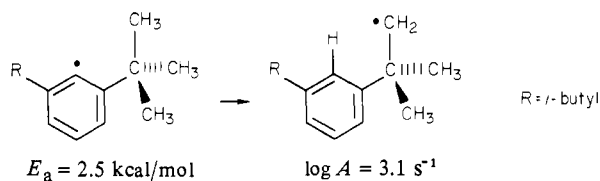


X-ray crystallography reveals that photochemical loss of nitrogen produces DPC perfectly oriented with respect to **9** for cycloaddition. The crystal enforced ideal geometry results in an extremely high $\log A$ value for this reaction site.

The physical significance of rate constants is much more apparent in units of s^{-1} rather than $\text{s}^{-1/2}$. Accordingly, the decay kinetics of DPC were analyzed over a small time interval over which the $\log I$ vs. time plot was linear. Acceptable accuracy and precision were achieved by analyzing the initial 20% of DPC decay following photolysis (see Figure 3). The initial pseudo-first-order decay rate constants are listed in Table II; the Arrhenius parameters appear in Table III. The Arrhenius parameters are extremely low and are highly reminiscent of the values obtained by Williams for matrix isolated methyl radical,²³ and by Ingold and Griller for sterically hindered phenyl radicals.²⁴



$$E_a = 0.9 \text{ kcal/mol}; \log A = 0.041 \text{ M}^{-1} \text{ s}^{-1}$$



The extremely low Arrhenius parameters observed in this work, and by others, are diagnostic of hydrogen atom transfer by quantum mechanical tunneling.²⁵ The isotope effects on the Arrhenius parameters support this interpretation. According to

Table II. Experimental and Calculated Pseudo-First-Order Initial Rate Constants

matrix	temp, K	$k_{\text{exptl.}} \text{ s}^{-1}$	$k_{\text{calcd.}} \text{ s}^{-1}$
methylcyclohexane	120	0.0022	0.0026
	114	0.0013	0.0011
	117	0.0019	0.0016
	111	0.00061	0.00074
	108	0.00053	0.00052
methylcyclohexane- d_{14}	123	0.0022	0.0027
	120	0.0018	0.0016
	117	0.0014	0.00098
	114	0.00046	0.00062
	111	0.00042	0.00041
benzene	141	0.0028	0.0029
	137	0.0016	0.0016
	133	0.00068	0.00088
	127	0.00045	0.00039
	121	0.00022	0.00019
benzene- d_6	145	0.0040	0.0028
	141	0.0015	0.0017
	137	0.00072	0.00099
diethyl ether	133	0.00049	0.00061
	127	0.00042	0.00031
	93	0.063	0.044
	90	0.017	0.022
	87	0.0087	0.011
diethyl ether- d_{10}	77	0.0022	0.0019
	98	0.073	0.052
	94	0.017	0.016
	91	0.0038	0.0063
	77	0.00019	0.00017
2-propanol	110	0.0097	0.013
	106	0.0066	0.0062
	102	0.0045	0.0031
	77	0.00017	0.00019
	77	0.00063	0.00073
toluene	95	0.0046	0.0036
	99	0.0067	0.0060
	103	0.0095	0.011
	106	0.017	0.018
	119	0.015	0.016
toluene- d_8	115	0.0088	0.0083
	111	0.0045	0.0044
	107	0.0032	0.0025
	104	0.0014	0.0017
	91	0.031	0.031
cyclohexene	87	0.014	0.014
	77	0.0036	0.0036
	100	0.024	0.026
	97	0.011	0.015
	94	0.0092	0.0088
cyclohexene- d_{10}	87	0.0078	0.0031
	77	0.0006	0.0011

Table III. Initial Pseudo-First-Order Arrhenius Parameters

matrix	E_a , kcal/mol	$\log A$, s^{-1}	A_D/A_H
toluene	2.1	2.4	
toluene- d_8	3.1	3.6	16
diethyl ether	2.9	5.4	
diethyl ether- d_{10}	4.0	7.4	100
2-propanol	2.3	2.6	
benzene	4.3	4.1	
benzene- d_6	5.3	5.4	20
methylcyclohexane	2.8	2.3	
methylcyclohexane- d_{14}	3.6	3.6	20
cyclohexene	3.2	2.0	
cyclohexene- d_{10}	4.5	2.7	20

classical transition-state theory $A_D/A_H \leq 2.26$. Values of $A_D/A_H = 100$ have been observed and require a tunneling interpretation. These conclusions are rendered somewhat less than straightforward by the possibility of site problems complicating the data. Objections of this type, the basis of the tunneling interpretation, and

(22) Doetschman, D. C.; Hutchison, C. A., Jr. *J. Chem. Phys.* **1972**, *56*, 3964.

(23) (a) Campion, A.; Williams, F. *J. Am. Chem. Soc.* **1972**, *94*, 7633; (b) Wang, J. T.; Williams, F. *Ibid.* **1972**, *94*, 2930; (c) LeRoy, R. J.; Sprague, E. D.; Williams, F. *J. Phys. Chem.* **1972**, *76*, 546.

(24) Brunton, G.; Griller, D.; Barclay, L. R. C.; Ingold, K. U. *J. Am. Chem. Soc.* **1976**, *98*, 6803.

(25) Bell, R. P. "The Tunnel Effect in Chemistry"; Chapman and Hall: New York, 1980.

(26) Bigeleisen, J. *J. Phys. Chem.* **1952**, *56*, 823.

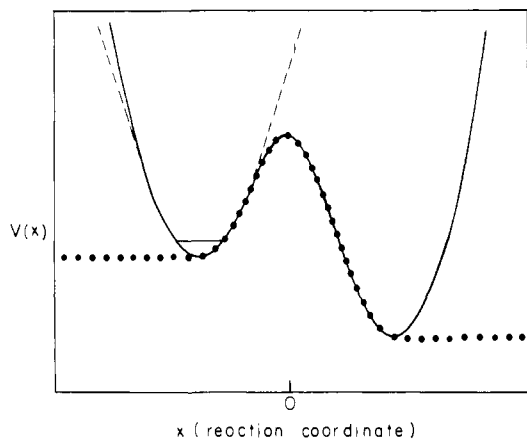


Figure 4. Schematic of the potentials involved in the theoretical model: (—) the exact potential along the reaction path; (---) the harmonic approximation to the reactant C-H stretch; and (···) the approximate barrier potential.

further evidence of multiple sites are discussed in the following two sections.

Procedure for Quantum Mechanical Calculations of Tunneling Rates

A simple extension of transition-state theory was recently outlined by LeRoy et al.²⁷ which, as they have demonstrated, adequately describes the rate of hydrogen atom abstraction by tunneling in low-temperature solids. It is this theory, essentially without modification, that we have used to interpret the hydrogen abstraction reactions of diphenylcarbene in six glassy matrices at low temperature. We will first briefly describe the principal ideas of this simple theory and then present the working equations in the form in which we employed them to obtain potential barriers for tunneling in each system. It is important to take note of the underlying assumptions of the theory in assessing the validity of the potentials so obtained. These calculations do not convert measurements of the rate constants, $k(T)$, into quantitative measurements of potential energy functions, but our work and that of LeRoy et al.²⁷ indicates that the potentials obtained from this model can show chemically significant trends.

The components of the model are suggested by the sketch of the potentials in Figure 4. We begin with the assumption that the abstraction reaction can be represented as the motion of the hydrogen atom in one dimension along a linear path.²⁸ In Figure 4 the solid curve represents the double well potential which is the potential energy as a function of the hydrogen atom's position, x , along the reaction path. This potential can be thought of as the cut along the reaction path of the complete potential energy hypersurface which is a function of the positions of all the atoms in the reacting system. However, since lattice vibrations, internal rotations, and other motions are coupled to the C-H stretching vibration, we cannot ignore those motions entirely and succeed in correctly predicting the temperature dependence of the rate, $k(T)$.

In general, the rate constant can be written as the Boltzmann average of the microcanonical rate, $k(E)$

$$k(T) = \frac{\sum_E k(E)g(E)e^{-E/k_B T}}{\sum_E g(E)e^{-E/k_B T}} \quad (1)$$

where $g(E)$ is the total degeneracy of the system at energy E and k_B is Boltzmann's constant. To exhibit the ideas underlying the model, we will describe how each component of the exact and

general expression in eq 1 is evaluated approximately. A central assumption is that $k(E)$ can be approximated by the transition-state theory expression

$$k(E) = \nu(E)P(E) \quad (2)$$

where $\nu(E)$ is the frequency of the C-H stretch and $P(E)$ is the barrier transmission probability at energy E . Equation 2 can be interpreted as follows. The frequency, $\nu(E)$, is the number of times per second that the hydrogen atom reaches the barrier through which it must tunnel to react, and $P(E)$ is the probability that, in any one encounter, the hydrogen atom tunnels through the barrier to the products region. The product of $\nu(E)$ and $P(E)$ gives $k(E)$ in units of s^{-1} .

A further important assumption of the model is that the total energy E is the sum of the energy of the C-H vibrational states, ϵ_n , and the contribution, E_c , which is considered to be a continuum due to all other motions.

$$E = \epsilon_n + E_c \quad (3)$$

The coupling of lattice vibrations, etc., to the C-H stretch is introduced by the device of eq 3 because now the tunneling probability will appear as $P(\epsilon_n + E_c)$. In this way an energetic continuum (weighted by the Boltzmann factor) is associated with each vibrational level of the C-H stretch and we may crudely picture this the "smearing out" of these vibrational levels due to coupling of other degrees of freedom. The fact that E_c is considered to be a continuum is critical because it is from this assumption that most of the temperature dependence of $k(T)$ will arise.

After this partitioning of the energy, eq 1 becomes²⁹

$$k(T) = \left[\sum_{n=0}^{\infty} \nu(n) e^{-\epsilon_n/k_B T} \int_0^{\infty} dE_c P(\epsilon_n + E_c) \rho(E_c) e^{-E_c/k_B T} \right] / \left[\sum_{n=0}^{\infty} e^{-\epsilon_n/k_B T} \int_0^{\infty} dE_c \rho(E_c) e^{-E_c/k_B T} \right] \quad (4)$$

where $\rho(E_c)$ is the density of states for all degrees of freedom except the C-H stretch. This expression is simplified by three further assumptions. (1) The vibrational motion in the C-H stretch is harmonic (dashed potential in Figure 4) so the vibrational frequency is independent of n and the vibrational energy levels are those of the harmonic oscillator.

$$\nu(n) = \nu \quad (5)$$

$$\epsilon_n = (n + 1/2)h\nu$$

(2) The density of states, $\rho(E_c)$, is unity, independent of energy. (3) $P(E)$ is the transmission probability of a simple potential barrier like the one represented by the dotted line in Figure 4.

With these assumptions the sums in eq 4 can be performed (after some rearrangement of the integrals in the numerator) to give the final working equation

$$k(T) = \frac{\nu}{k_B T} (1 - e^{-h\nu/k_B T}) \int_{\epsilon_0}^{\infty} P(E)F(E)e^{-(E - \epsilon_0)/k_B T} dE \quad (6)$$

where ϵ_0 is the zero point energy of the C-H stretch ($h\nu/2$) and $F(E)$ is the number of vibrational states of the C-H stretch with energies $\epsilon_n = (n + 1/2)h\nu \leq E$.

All that remains is the choice of the barrier potential, $V(x)$, which defines transmission probability $P(E)$. LeRoy et al.²⁷ found that the model expressed by eq 6 is insensitive to minor details of $V(x)$. We have chosen the Eckart barrier³⁰ given by

$$V(x) = -(V_1 - V_2)y/(1 - y) - (V_1^{1/2} + V_2^{1/2})^2 y/(1 - y)^2 \quad (7)$$

where $y = -e^{x/a}$. Some plots of Eckart barriers for various values

(29) LeRoy et al. in ref 27 also allow for the possibility that not all the energy, ϵ_n , of vibration is available along the reaction path. However, since they obtained best results without this embellishment, we have ignored it here.

(30) Eckart, C. *Phys. Rev.* **1930**, *35*, 1303. See also Johnston, H. S. "Gas Phase Reaction Rate Theory"; Ronald Press: New York, 1966; p 42. Note that there are several errors in Johnston's expressions for the transmission probability. Eckart's expressions are correct.

(27) LeRoy, R. J.; Murai, H.; Williams, F. *J. Am. Chem. Soc.* **1980**, *102*, 2325.

(28) The (presumably small) effects of curvature of the reaction path could be incorporated in the barrier permeability $P(E)$.

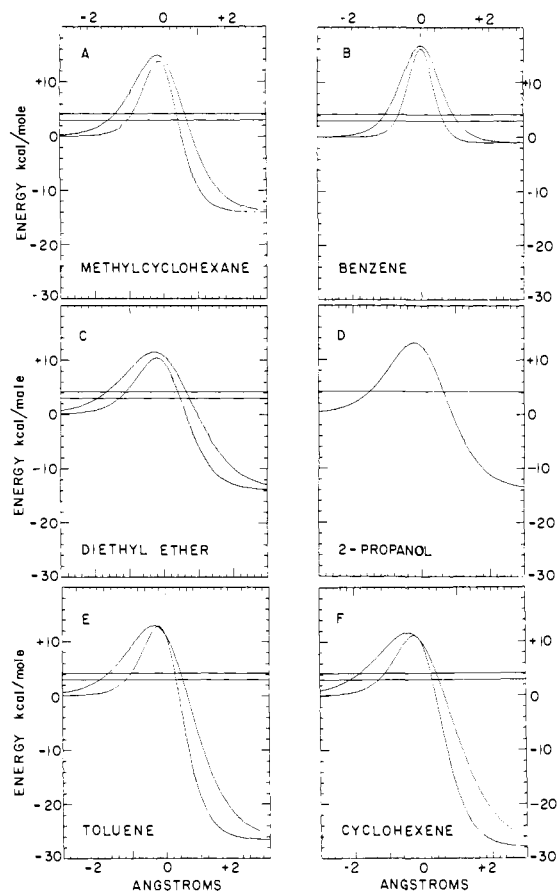


Figure 5. Eckart potentials found for each matrix and its deuterated form. See text for explanation of differences. Horizontal lines indicate zero point energies. The 2-propanol- d_8 matrix was not fit, as product studies indicate that the chemistry in this matrix is largely a singlet DPC process.

of the parameters can be seen in Figure 5. The advantages of using this form for the potential barrier are that the probability function $P(E)$ is known exactly as a simple analytic expression³⁰ and that it can be parameterized with only two parameters as follows. The exothermicity, ΔH , of the reaction is given by $\Delta H = (V_1 - V_2)$. Since the exothermicity is a fixed and usually known quantity, LeRoy et al.²⁷ did not use it as a variable in the analysis and we have done likewise. Therefore the potential is parameterized entirely by two variables: a_1 , which is related to the barrier width, and V_1 , which is related to the barrier height. It is these two parameters which we extract from the experimental values of $k(T)$. The reaction exothermicity does not appreciably affect the computed values of V_1 and a_1 . Changing ΔH by ± 2 kcal changes the computed values of V_1 by less than 1%. In simple terms, as soon as the tunneling hydrogen atom emerges on the product side of the barrier it is very rapidly vibrationally deactivated.³¹ Therefore, the tunneling rate constant is not sensitive to ΔH for an exothermic reaction, as there will be no reverse endothermic tunneling through the barrier. Values of ΔH were chosen based on analogies to free radical processes, for which bond dissociation data are available.³²

The values of V_1 and a_1 were computed by performing a nonlinear least-squares fit of $k(T)$ from eq 6 to the observed rate constants, $k_{\text{obsd}}(T)$, with a procedure which can be summarized

as follows. First, choose values for the ϵ_0 and ΔH from spectroscopic and thermodynamic data. These are nonadjustable parameters. Then, by varying V_1 and a_1 , minimize the value of the weighted sum of squares of deviations

$$\chi^2 = \sum_i [\log(k_{\text{obsd}}(T_i)) - \log(k(T_i))]^2 / u_i^2 \quad (8)$$

where u_i^2 is the sum of the squared uncertainties in the experimental value of $\log(k_{\text{obsd}}(T_i))$ and the value computed from eq 6 for $\log(k(T_i))$, at the temperature T_i .

This procedure was followed for all six matrices and their deuterated forms. In the calculations on the deuterated matrices the value of ϵ_0 was changed to that appropriate for the C-D stretch. Only one minimum was detected in the nonlinear least-squares minimization in all cases.

Based on the precedent of LeRoy et al.,²⁷ we have associated ϵ_0 with an asymmetric stretching vibration. This is a somewhat arbitrary assumption for DPC, as conceivably the reaction coordinate may resemble a bending vibration. Accordingly, we have arbitrarily used a zero point energy of 3000 cm^{-1} (4.2 kcal/mol) for all six matrices. Changing the zero point energy by $\pm 100 \text{ cm}^{-1}$ changes V_1 and a_1 by less than 2%. Reducing the zero point energy by a factor of 3 will decrease both V_1 and a_1 without affecting the quality of the data fitting or changing the qualitative conclusions.³³

A final comment on the interpretation of the values of V_1 and a_1 obtained in this fashion is in order. The barrier height is *not* V_1 . Instead, the value of the Eckart potential, $V(x)$, at $x = 0$ is the barrier height and is given by eq 7 as

$$V(0) = V_1 \left(1 + \left(1 - \frac{\Delta H}{V_1} \right)^{1/2} \right) / 2 + \Delta H / 4 \quad (9)$$

which reduces to V_1 only if $\Delta H = 0$. Also, it should be noted that a_1 is not the distance over which the hydrogen or deuterium must tunnel. That distance varies with the energy in question. A value of the tunneling distance at the zero point energy of vibration can be read off from Figure 5 and, since most of the contribution to the Boltzmann average in eq 6 comes from energies near ϵ_0 at low temperatures, the tunneling distance at that energy is a reasonable value to associate with each system.

Results and Discussion

The rate constants calculated by least-squares minimization are listed in Table II along with the experimental values. The agreement is extremely good and comparable to that observed by LeRoy et al.²⁷ where site problems seem much less severe. The tunneling calculations have two consequences of immediate importance. In six matrices of widely varying chemistry, the decay of triplet DPC is consistent with hydrogen atom abstraction via a tunneling mechanism. This is true even in cyclohexene, where carbene addition to the double bond is an attractive alternative. The good quality of the data fitting is consistent with a "singlet site" interpretation. By this we mean that the initial decay rates correspond to the same reaction site (identical barrier heights and widths) at the low and high ends of the temperature regimes studied. This would mean that the low Arrhenius parameters of Table III reflect tunneling reactions rather than multiple site problems. The ability to detect the kinetics of the same site within a 20–30 K temperature interval reflects the small variation in tunneling rate relative to a classical process within this temperature regime. It is conceivable that the high- and low-temperature ends of the kinetic studies correspond to very different matrix sites. If this is true then the success of the model is fortuitous, and the measured A values are artificially low. We cannot definitively rule out this possibility. However, at the present time there is no compelling reason to invoke a multiple site problem, over a narrow temperature range, in the abbreviated kinetic interval.

The least-squares fit tunneling height (V_1) and width (a_1) parameters are listed in Table IV. The barrier height $V(0)$ can

(31) The rate of vibrational relaxation by radiationless transitions usually occurs on a subnanosecond time scale in the condensed phase. See Turro, N. J. "Modern Molecular Photochemistry"; Benjamin and Cummings: Menlo Park, CA, 1978.

(32) ΔH can be estimated for $\text{Ph}_2\text{C} + \text{RH} \rightarrow \text{Ph}_2\dot{\text{C}}\text{-H} + \text{R}\cdot$ from $\Delta H = \text{B.D.E.}(\text{RH}) - \text{B.D.E.}(\text{Ph}_2\dot{\text{C}}\text{-H})$. The bond dissociation energy of $\text{Ph}_2\dot{\text{C}}\text{-H}$ is not known, but it was assumed to be equal to benzene (110 kcal/mol) as in each case it is an sp^2 C-H bond that is broken. The B.D.E. data for RH were taken from Benson in ref 14.

(33) Changing ϵ_0 from 3000 to 1000 cm^{-1} for the toluene matrix reduces V_1 from 13.2 to 10.91 kcal/mol and a_1 from 1.28 to 0.96 \AA .

Table IV. The Eckart Potential Parameters V_1 and a_1 Obtained from Least-Squares Minimization. Energies Are in kcal

matrix	V_1	$a_1, \text{\AA}$	$-\Delta H$	ϵ_0	$V(0)$	χ^2	N
methylcyclohexane	14.8	1.04	14	4.174	14.2	0.022	5
methylcyclohexane- d_{14}	13.7	0.694	14	2.951	13.1	0.051	5
benzene	16.7	0.783	1	4.174	16.7	0.014	5
benzene- d_6	16.2	0.429	1	2.951	16.2	0.072	5
diethyl ether	11.4	1.37	14	4.174	10.7	0.051	4
diethyl ether- d_{10}	10.4	0.940	14	2.951	9.6	0.075	4
2-propanol	13.2	1.18	14	4.174	12.5	0.052	4
toluene	12.9	1.25	26.58	4.174	11.1	0.023	5
toluene- d_8	12.8	0.766	26.58	2.951	11.0	0.021	5
cyclohexene	11.6	1.43	28	4.174	9.5	0.00035	3
cyclohexene- d_{10}	11.1	0.879	28	2.951	9.0	0.24	5

be converted into a classical activation energy by subtracting an unknown portion of the zero point energy (4.2 kcal/mol for H, 2.8 for D). These results indicate that there may be a substantial activation energy in solution (6–12 kcal/mol) to triplet hydrogen atom abstraction. The trends observed in $V(0)$ are generally consistent with chemical intuition based on bond dissociation energies. Benzene, which is the poorest hydrogen atom donor, has by far the largest energy barrier to reaction. This is followed by the unactivated alkane methylcyclohexane. Two of the lowest barrier heights observed are with toluene and cyclohexene. This is as expected due to the resonance stabilization of the resultant benzyl and cyclohexenyl radicals. Curiously, diethyl ether has the lowest barrier height. Only when benzene matrices are employed will all of the matrix C–H bonds have identical bond dissociation energies and identical V_1 's for a given orientation. Product studies of Tomioka and Moss indicate that triplet carbene abstraction occurs largely but not necessarily exclusively at the weakest C–H bond. For toluene and cyclohexene assuming that abstraction occurs only from a benzylic or allylic C–H bond with a unique value of V_1 for that site is undoubtedly valid. The assumption that only one type of C–H bond, with a unique V_1 , suffers abstraction in the site of interest is less valid for diethyl ether and 2-propanol but it will be employed in the absence of more complete information and the interests of simplicity. The rate data for 2-propanol- d_8 was not fit as product studies reveal that the chemistry in this matrix is largely a singlet process. LeRoy and Williams found²⁷ that the potentials calculated for the reactions of methyl radical were somewhat higher than the values measured in solution. This effect might also be true for the calculated DPC potentials of this work. It is likely that the solid-state environment forces the reaction along a less than ideal reaction coordinate, such as would be traversed in solution.

A very clear trend in barrier widths is apparent in Table IV and Figure 4. In every matrix the barrier widths are dramatically reduced upon perdeuteration. A single site is monitored in both the protio and deuterio matrices, but they are not the same sites! The observed deuterio sites are more reactive than the observed protio sites. The k_h/k_d ratios of Table I must be considered the minimum isotope effects as one is comparing slow proton sites against fast deuterium sites. In order to obtain a signal large enough for kinetic analysis, the diphenyldiazomethane-containing matrix is irradiated for 100 s to build up the concentration of DPC. During the course of photolysis all types of matrix sites are created from extremely fast to inert (see Figure 6). In the protio matrix the most reactive sites are photochemically populated and thermally depleted by reaction prior to shuttering the lamp. Sites such as A and B are presently invisible within the time resolution of the system. Deuteration of the matrix produces a large rate retardation. The protio sites such as A and B which were too fast to study are brought into a measurable range by the isotope effect. The previously measured sites in the protio matrix such as C will appear inert in the deuterio matrix. The respective Arrhenius parameters of Table III for proton and deuterium-containing matrices are not associated with the same matrix site either. We should emphasize that LeRoy et al.²⁷ have established the limits of reliability of the theoretical model to the extent that the differences we observe in the potential parameters a_1 and V_1 between the sites seen in the protio and deuterio matrices are clearly

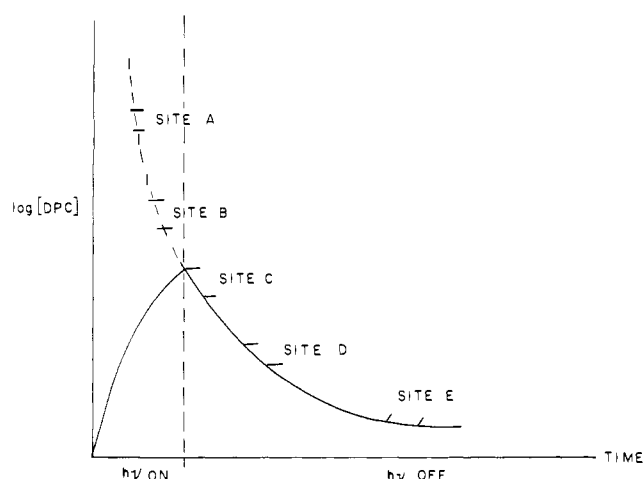


Figure 6. While the sample is irradiated the DPC signal grows as sites of widely varying reactivity are created. The signal decays as soon as the light source is shuttered. The dashed line idealizes the signal decay of very reactive sites which were not time resolved. The brackets represent small linear portions of the decay curve which are associated with the unique rate constant for a specific site.

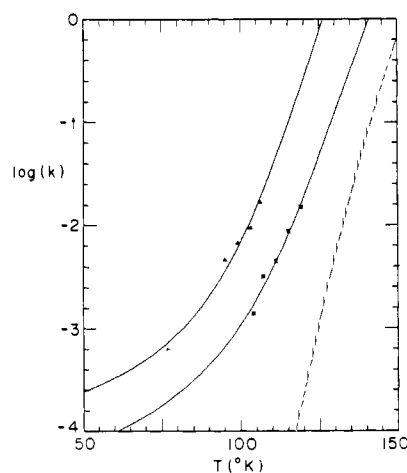


Figure 7. Predicted isotope effect for identical matrix sites. The log of the rate constant computed from E_a (6) is shown by the solid line passing through the experimental rate constants for toluene (Δ) and toluene- d_8 (*). The dashed line is the toluene- d_8 rate predicted by the parameters of the toluene matrix.

significant. The least-squares fit is so sensitive that 5% changes in a_1 or V_1 in the case of the toluene matrix, for example, change the rate at 100 K by factors of 2.7 and 12, respectively.

From results on hydrogen abstraction reactions LeRoy et al.²⁷ predict isotope effects of as much as 12 orders of magnitude at low temperatures. Using the separate results of our analyses of the protio or deuterio matrices we predict similar isotope effects. At 4 K, k_h/k_d is predicted to be 10^4 . The evidence that our results on the protio and deuterio sites represent different sites is illustrated by the comparisons in Figure 7. The isotope effect predicted from

the results on the protio matrix in the example shown there is far greater than that observed experimentally, but close fits to the experimental data for the two matrices are obtained using different sites for the two cases.

The Implications of the Tunnel Effect for Matrix Chemistry

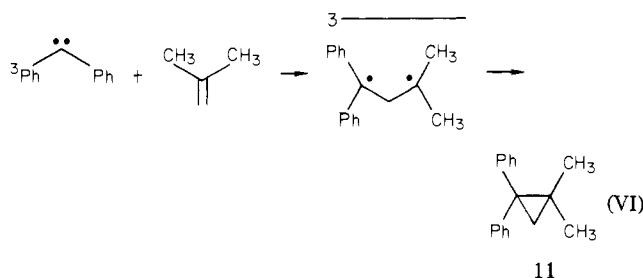
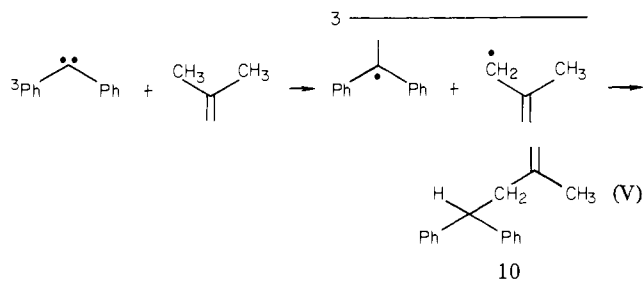
With hindsight it is not surprising that the matrix reactions of triplet DPC can proceed by tunneling in preference to classical hydrogen atom abstraction and addition to unsaturated bonds. At the present time no one has measured the solution Arrhenius parameters for any triplet carbene abstraction or addition process. Based upon analogous free radical processes,³⁴ one can estimate that $\log A$ and E_a will fall in the ranges $8-11 \text{ M}^{-1} \text{ s}^{-1}$ and $6-12 \text{ kcal/mol}$, respectively. If one simply ignores the phase changes which occur between 273 and 77 K and uses the most optimistic Arrhenius parameters ($\log A = 11 \text{ M}^{-1} \text{ s}^{-1}$, $E_a = 6 \text{ kcal/mol}$), the calculated rate constant at 77 K is less than $10^{-6} \text{ M}^{-1} \text{ s}^{-1}$. In the absence of tunneling, triplet carbene reactions in matrices at 77 K should not occur!

One of the earliest documentations of tunneling in an organic reaction was by Lewis and Funderburk.³⁵ These workers studied proton transfer from 2-nitropropane to sterically hindered pyridines. It was pointed out that steric hindrance in the reagents produced a tall thin barrier through which tunnel effects should be maximal. McBride has likened the effect of the matrix on a solid state reaction to a "super steric effect".³⁶ The rigidity of the matrix environment prevents solution-like diffusion and rotation of DPC and a matrix molecule, thereby further decelerating a classical reaction.

A large portion of the chemistry in 77 K matrices takes place too fast to be monitored kinetically with the present equipment. It is an open question whether tunneling is important in the fast, invisible matrix sites.

However, not all of the products observed in matrix reactions arise by hydrogen atom tunneling. When olefinic matrices are employed, triplet DPC can react by hydrogen atom abstraction-recombination (V) or by addition cyclization (VI). Moss has found that the ratio of **10**:**11** varies from 0.2 to 44 between 273 and 77 K.⁷ The matrix kinetic isotope effects observed with cyclohexene-*d*₁₀ at 77 K ($k_H/k_D = 6$) are consistent with the isobutylene chemistry. Given a choice between allylic hydrogen atom abstraction or addition to a double bond in a matrix at 77 K, the former process is substantially preferred. This is a consequence of tunneling and not a consequence of the respective Arrhenius parameters of the abstraction and addition pathways. Although it is conceivable that cyclopropanes can be formed by heavy atom tunneling,³⁷ this does not seem likely in the rigid matrix. Rapid crystallization of olefinic matrices produces a myriad of orientations of diazo compound relative to alkene. It is likely that in a small percentage of the sites the diazo orientation might resemble

the orientation of **1** relative to diphenylethylene studied previously in a single crystal by Doetschman and Hutchison.²² The nascent carbene is generated directly over the carbon-carbon double bond and can react by addition with minimal motion in the matrix. It is possible that the addition reactions in idealized matrix sites occur too fast for observation.



Conclusions

The decay kinetics of triplet DPC in low-temperature matrices can be measured by ESR. The decay reaction is attributed to triplet hydrogen atom abstraction from the matrix based on product studies and chemical and kinetic isotope effects. The nature of the isotope effects indicates that the reaction proceeds by hydrogen atom tunneling. Asymmetric Eckart barrier calculations can reproduce the experimental rate constants and give reasonable values of the barrier height and width parameters.

Experimental Section

The low-temperature ESR kinetic system has been described previously.^{9,10} Diphenyldiazomethane was prepared by oxidation of the corresponding hydrazone as described in the literature.^{7,8} Authentic samples of diphenylcarbene adducts with 2-propanol were synthesized as described in the literature.³⁷ The 2-propanol reaction mixtures were analyzed on a 5830 Hewlett-Packard gas chromatograph using a 6-ft 5% SE 30 column at 147 °C. The identities of the reaction products were verified by GC-mass spectroscopy and by coinjection with authentic samples. All deuterated solvents were purchased from Merck Sharp and Dohme and used without purification. The undeuterated solvents were distilled over calcium hydride prior to use. Sample tubes were sealed under vacuum after three freeze-thaw cycles in 4-mm quartz (ESR work) or Pyrex (GC work) tubes. A 1000-W xenon lamp was used in the ESR work in conjunction with copper sulfate filters. A Rayonet Reactor with 16 RPR-3500 Å lamps was used for product studies. The sample tubes were immersed in a glass Dewar filled with liquid nitrogen and irradiated for 1.5 h. The tubes were kept in liquid nitrogen for 48 h prior to thawing. Acrylonitrile was added to the samples to consume unreacted diphenyldiazomethane. The sample was allowed to stand for 30 min prior to GC analysis.

Acknowledgment. The authors gratefully acknowledge support of this work by the National Science Foundation. We also wish to thank Professor Hideo Tomioka for details of the synthesis of the DPC-2-propanol adducts and for the generous gift of microsamples for use in VPC identification. M.S.P. wishes to thank E. I. du Pont de Nemours & Company for a young faculty grant.

Registry No. **1**, 883-40-9; DPC, 3129-17-7; D₂, 7782-39-0.

(34) See Ingold, K. U. in "Free Radicals"; Vol. I, Kochi, J., Ed.; Wiley: New York, 1973.

(35) Lewis, E. S.; Funderburk, L. H. *J. Am. Chem. Soc.* **1967**, *89*, 2322.

(36) (a) McBride, J. M. *J. Am. Chem. Soc.* **1971**, *93*, 6302; (b) Jaffe, A. B.; Skinner, K. J.; McBride, J. M. *Ibid.* **1972**, *94*, 8510; (c) Jaffe, A. B.; Malament, D. S.; Slisz, E. P.; McBride, J. M. *Ibid.* **1972**, *94*, 8515; (d) Tremelling, M. J.; McBride, J. M. *J. Org. Chem.* **1972**, *37*, 1073; (e) Skinner, K. J.; Blaskiewicz, R. J.; McBride, J. M. *Isr. J. Chem.* **1972**, *10*, 457. Other descriptions of solid state chemistry can be found in Schmidt, G. M. J., et al. "Solid State Photochemistry"; Verlag-Chemie: Weinheim, D.D.R., 1976; and Scheffer, J. R. *Acc. Chem. Res.* **1980**, *13*, 283.

(37) (a) Banger, J.; Jaffe, A.; Lin, A.-C.; Saunders, W. H., Jr. *J. Am. Chem. Soc.* **1975**, *97*, 7177; (b) Wilson, J. D.; Kallsson, I.; Saunders, W. H., Jr. *Ibid.* **1980**, *102*, 4780; (c) Buchwalter, S. L.; Closs, G. L. *Ibid.* **1979**, *101*, 4688.

(38) (a) Olson, W. T.; Hipsher, H. F.; Buess, C. M.; Goodman, I. A.; Hart, I.; Lamneck, J. H., Jr.; Gibbons, L. C. *J. Am. Chem. Soc.* **1947**, *69*, 2451; (b) Bornstein, J.; Nunes, F. J. *J. Org. Chem.* **1965**, *30*, 3324; (c) Easton, N. R.; Fish, V. B. *J. Am. Chem. Soc.* **1947**, *69*, 2451.